South East Asian J. of Mathematics and Mathematical Sciences
Vol. 16, No. 2 (2020), pp. 195-218

ISSN (Online): 2582-0850

ISSN (Print): 0972-7752

HYDRODYNAMIC LUBRICATION OF SYMMETRIC ROLLERS WITH TWO DIMENSIONAL CONSISTENCY VARIATION OF POWER LAW FLUIDS

Jalatheeswari N, Dhaneshwar Prasad and Venkata S Sajja*

Department of Mathematics,
Kanchi Mamunivar Centre for Post Graduate Studies,
Airport Road, Lawspet, Puducherry - 605008, INDIA

E-mail : njalatheeswari@gmail.com, rpdhaneshwar@gmail.com

*Department of Mathematics,
Koneru Lakshmaiah Education Foundation,
Guntur - 522502, Andhra Pradesh, INDIA

E-mail : njalatheeswari@gmail.com

(**Received:** *Oct. 16, 2019* **Accepted:** *Jul. 21, 2020* **Published:** *Aug. 30, 2020)*

Abstract: Roller bearing is one among the varieties of rotating system incorporating the forces between a system and its environment. It also guides the movement of rotation smoothly, and hence, rolling bearings are significant machine elements pertaining to the lifetime of the system and its accuracy. Here, a thick fluid lubrication of rollers along with normal squeezing motion is considered. The consistency variation of power law lubricant on temperature and pressure is taken into account. A specific model for the lubricant consistency is considered to vary along and across the flow directions. Load, traction, temperature and pressure are calculated for various values of the consistency index n and normal velocity q. These are matched well with the previous results.

Keywords and Phrases: Hydrodynamic lubrication, non-Newtonian power law, Consistency variation, Thermal effects, Normal Squeezing, Cylindrical roller bearings.

2010 Mathematics Subject Classification: 76N02.

1. Introduction

The utility of roller bearing to this modern world is bountiful. Its main function is to transmit the load at very low friction. At normal loads, the bearings do experience normal pressure and temperature. At heavy load and high speed, the bearings experience the Himalayan pressure and temperature. In squeezing motion, this pressure and temperature is even more. Here comes the necessity for the application of squeeze-film technology to optimize the pressure and temperature.

Reynolds equation influenced its power to investigate film thickness, viscosity, and density. These properties are temperature and pressure dependent. Cope in 1949, included some changes to classical Reynolds equation like adding viscosity and density variation with fluid flow. All these changes are included to exhibit energy equation responsible for the temperature in the film. He put together continuity equation and energy balance equation in the fluid film to create temperature and pressure distribution. In this connection, researchers attempted to develop an intelligible model. Dowson successfully studied such cases and concluded that the viscosity of Newtonian fluid does not change much in a lightly loaded system. However, in heavily loaded system, such character of the fluid may not be true [1]. Rong-Tsonn and Hamrock [2], made a detailed study on compressibility and squeezing of isothermal Newtonian lubrication. To serve a single non-dimensional squeeze Reynolds number, Usha and Sridharan [3] examined a laminar squeezing flow of an incompressible Newtonian fluid between plane annuli.

Further Cheng and Sternlicht [4] analysed EHD rolling/sliding line contact problem and obtained solutions for equation of motion and heat transfer equation considering viscosity to be a function of x and y both. Ghosh and Hamrock [5] also solved such problem using finite difference method while analyzing the film shape by subjecting each rectangular area to a uniform pressure. Unlike Hertzian pressure, the temperature there was not found to be continuous. However, in both cases, squeezing effects were ignored.

Primarily lubricants staged a different character at shear stresses and high pressure. Secondly, Newtonian behavior is seldom exhibited in fluids such as molten plastic, slurries and pulps. Besides, the presence of high molecular weight polymers earns them the label of non-Newtonian. Within the general framework of non-Newtonian fluids, the power law model was more attractive. Prasad et al. [6] exposed the consistency variation of power law fluids with temperature and pressure and displayed how the pressure peak is dragged away from the center line of contact by temperature influence. The trend was found exactly opposite to that of cavitated points.

A semi solid substance like grease is one of the most used non Newtonian lubri-

cants. Neurouth et al. [7] proposed a thermal model for grease-lubricated thrust ball bearings. Here, thermal network method was utilized to study the temperature distribution. In addition, the bearings' power loss was calculated numerically, and concluded that the bearing's inner temperature distribution has minimum effect because of heat convection. Ai et al. [8] developed a feasible thermal model for a grease lubricated double-row tapered bearing by capitalizing Ohm's law to describe the behavior of Herschel – Bulkley model. Various heat sources like: frictional heat dissipation between roller's large end, frictional heat of roller race-way contact, roller's viscous drag loss, raceway flange contact, were incorporated within the model. The increase in speed and grease filling ratio increases the bearing's temperature. This is clearly evident from their numerical results. Yan et al.[9] model aimed to measure the roller inner ring flange contact of tapered roller bearing and roller raceway contact used in super speed train. It concluded that inner ring flange receives highest temperature [10]. Viscosity variation because of temperature and pressure was presented by Osterle and Saibel [11]. Cameron [12] analysed the variation of viscosity across the fluid film thickness. Recently, Prasad et al. [13, 14] proposed a solution to asymmetric rollers using power law fluids. However, consistency variation along y direction was not considered.

Further, the deep interaction between the rolling elements and fluid makes the flow complex inside the bearing cavity. This was presented by Gao et al. [15]. Later, Gao et al. [16] tried to demonstrate two phase flow behavior in roller bearings with under-race lubrication.

In continuation, the study of thermo-hydrodynamic lubrication for a heavily loaded rigid cylindrical line contact with incompressible power law fluids is the goal of this study including cavitations. It is assumed that the lubricant consistency varies with pressure and film temperature under thermal and isothermal boundaries. Under the said condition, the heat effect of the fluid is observed for the rolling with and without squeezing motion including lubricant consistency variation across the fluid flow direction. The modified energy and Reynolds equations are obtained and solved yielding temperature and pressure.

2. Nomenclature

α : pressure coefficient
β : temperature coefficient
h : film thickness
h_0 : minimum film thickness
k : thermal conductivity of the lubricant
m : lubricant consistency
m_0 : consistency at ambient pressure and temperature
p : hydrodynamic pressure
q : squeezing parameter
R : radius of cylinder
T : lubricant temperature
T_0 : ambient temperature
T_{Fh} : traction force
u : velocity of the lubricant in x-direction
U : velocity of the lubricant at y=h/2
v : velocity of the lubricant in y-direction
V : normal velocity (V/2) of either cylinder
x_1 : point of maximum pressure
x_2 : cavitation point

Subscripts: The subscript 1 and 2 denote respectively the corresponding quantities in the inlet and the outlet regions.

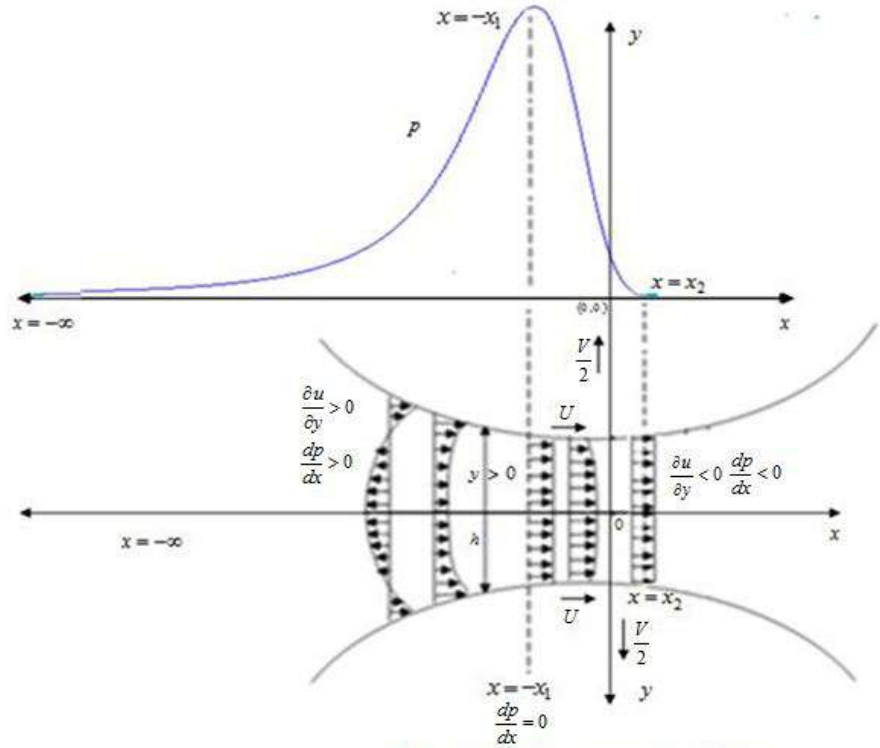

Fig.1: Lubrication of symmetric rollers

3. Mathematical Analysis

The governing equations for the one dimensional fluid flow are [17, 18]

$$\frac{\partial u}{\partial x} + \frac{\partial v}{\partial y} = 0 \tag{1}$$

$$\frac{dp}{dx} = \frac{\partial \tau}{\partial y} \tag{2}$$

$$k\frac{\partial^2 T}{\partial y^2} + \tau\frac{\partial u}{\partial y} = 0 \tag{3}$$

Where k is the thermal conductivity of the lubricant and is assumed to be constant,p is the hydrodynamic pressure, T being temperature due to heat dissipation; u and v are the velocities of the fluids in x and y directions respectively. τ, the shear stress relation for a non-Newtonian power law fluid is:

$$\tau = m \left|\frac{\partial u}{\partial y}\right|^{n-1} \frac{\partial u}{\partial y} \tag{4}$$

Where, the lubricant consistency m of the powerlaw fluid is assumed to vary as

$$m = m_0 \, e^{\alpha p - \beta (T - T_0)} \tag{5}$$

The boundary conditions for the system under consideration are:

$$\frac{\partial u}{\partial y} = 0 \; at \; y = 0; u = U at \; y = \frac{h}{2}; \tag{6}$$

The boundary conditions for the heat equation (3) are

$$\frac{\partial T}{\partial y} = 0 \; at \; y = 0; T = T_h \; at \; y = \frac{h}{2}; \quad where \; h = h_0 + \frac{x^2}{2R} \tag{7}$$

As the consistency m and temperature T being two dimensional, the equations (1) (2) and (3) cannot be solved analytically. Hence, an intuitive mathematical relationship for the consistency m is assumed to be [17]:

$$m = m_0 / \left(A_0 + A_1 y + A_2 y^2\right)^{n} \tag{8}$$

Where A_0, A_1andA_2 are functions of x only and are unknowns right now.
Integrating equation (1) with respect to 'y' with the assumed boundary conditions

(6), one can get for the region $-\infty < x \leq -x_1$

$$u_1 = U + [\frac{1}{m_0}(\frac{dp_1}{dx})]^{\frac{1}{n}}[\frac{nA_0}{n+1}(y^{\frac{n+1}{n}} - (\frac{h}{2})^{\frac{n+1}{n}}) + \frac{nA_1}{2n+1} (y^{\frac{2n+1}{n}} - (\frac{h}{2})^{\frac{2n+1}{n}}) + \frac{nA_2}{3n+1}(y^{\frac{3n+1}{n}} - (\frac{h}{2})^{\frac{3n+1}{n}})] \quad (9)$$

Similarly, for the region $-x_1 \leq x \leq x_2$, one can have

$$u_2 = U - [\frac{1}{m_0}(\frac{-dp_2}{dx})]^{\frac{1}{n}}[\frac{nA_0}{n+1}(y^{\frac{n+1}{n}} - (\frac{h}{2})^{\frac{n+1}{n}}) + \frac{nA_1}{2n+1} (y^{\frac{2n+1}{n}} - (\frac{h}{2})^{\frac{2n+1}{n}}) + \frac{nA_2}{3n+1}(y^{\frac{3n+1}{n}} - (\frac{h}{2})^{\frac{3n+1}{n}})] \quad (10)$$

Integration of the continuity equation (2) with the boundary conditions (6) together with the specified conditions: $v_{h/2} = \frac{U}{2}\frac{dh}{dx} + \frac{V}{2}$; $v_0 = 0$ at y =0 gives

$$\frac{\partial}{\partial x}\int_0^{h/2} u\, dy = -\frac{V}{2} \quad (11)$$

Further integration of the above equation with the assumed conditions:
$\frac{dp_1}{dx} = 0$ at $x = -x_1$ and $h = h_1$, one can get

$$\frac{dp_1}{dx} = m_0 \left(\frac{2}{h}\right) \left[\left(\frac{2}{h^2}\right) \frac{(U(h-h_1) + V(x+x_1))}{[\frac{nA_0}{2n+1} + \frac{nA_1}{3n+1}(\frac{h}{2}) + \frac{nA_2}{4n+1}(\frac{h}{2})^2)]}\right]^n ; -\infty < x \leq -x_1 \quad (12)$$

Similarly for the other region

$$\frac{dp_2}{dx} = -m_0 \left(\frac{2}{h}\right) \left[\left(\frac{2}{h^2}\right) \frac{-(U(h-h_1) + V(x+x_1))}{[\frac{nA_0}{2n+1} + \frac{nA_1}{3n+1}(\frac{h}{2}) + \frac{nA_2}{4n+1}(\frac{h}{2})^2)]}\right]^n ; -x_1 \leq x \leq x_2 \quad (13)$$

The constants, A_0, $A_1$and A_2, as mentioned in equation (8) , are calculated using the heat energy equation (3) with the boundary conditions mentioned in (7); and are obtained as:
$A_0 = 0$, $A_1 = 0$ and $A_2 = (4/h^2)\left(1/\overline{E}\right)^{\frac{1}{n}}$;
Making the above two equations dimensionless, these equations (12) and (13) are reduced to

$$\frac{d\overline{p_1}}{d\overline{x}} = \frac{\overline{m_0}\ \overline{E}\ \overline{f}^{\,n}}{\overline{h}^{\,2n+1}}; \quad -\infty < \overline{x} \leq -\overline{x_1} \quad (14)$$

$$\frac{d\overline{p_2}}{d\overline{x}} = - \frac{\overline{m_0}\ \overline{E}\ \overline{g}^{\,n}}{\overline{h}^{\,2n+1}};\ -\overline{x_1} \le \overline{x} \le \overline{x_2} \tag{15}$$

Where

$$\overline{x} = x/\sqrt{2Rh_0}; \overline{h} = h/h_0; \overline{g} = -\overline{f}; \overline{E} = e^{\overline{p}-\overline{T_h}+\overline{T_0}};$$
$$\overline{p} = \alpha p; \overline{m} = 2mc_n\alpha; \overline{f} = \overline{x}^{\,2} - \overline{x_1}^{\,2} + 2q\left(\overline{x} + \overline{x_1}\right);$$
$$q = (V/2U)\sqrt{2R/h_0};\ c_n = \left(2\left(4n+1\right)/n\right)^n \sqrt{2R/h_0}\,(U/h_0)^n;$$

Solving the energy equation (3) with the boundary condition given in (7), one can get in dimensionless

$$\overline{T_1} = \overline{T_h} - \frac{\overline{m_0}\ \overline{E}\,\overline{f}^{\,n+1}\,\overline{\gamma}\ \overline{l}}{\overline{h}^{\,\frac{2n^2+5n+1}{n}}};\ -\infty < \overline{x} \le -\overline{x_1} \tag{16}$$

$$\overline{T_2} = \overline{T_h} - \frac{\overline{m_0}\ \overline{E}\ \overline{g}^{\,n+1}\,\overline{\gamma}\ \overline{l}}{\overline{h}^{\,\frac{2n^2+5n+1}{n}}};\ -\overline{x_1} \le \overline{x} \le \overline{x_2} \tag{17}$$

where $\overline{\gamma} = \frac{\beta U h_0}{k\alpha}\sqrt{\frac{h_0}{2R}}$; $\overline{T} = \beta T$; $\overline{y} = y/h_0$; $\overline{l} = 2^{\frac{3n+1}{n}}\left(\frac{n}{5n+1}\right)\left(\overline{y}^{\frac{5n+1}{n}} - \left(\frac{\overline{h}}{2}\right)^{\frac{5n+1}{n}}\right)$;

Mean Temperature

The mean temperature T_m , defined as $T_m = \frac{2}{h}\int_0^{h/2} T\,dy$ is also calculated using the dimensionless scheme as

$$\overline{T_{m_1}} = \overline{T_h} + \frac{\overline{m_0}\ \overline{E}\,\overline{f}^{\,n+1}\,\overline{\gamma}\ d_n}{\overline{h}^{\,2n}};\ -\infty < \overline{x} \le -\overline{x_1} \tag{18}$$

$$\overline{T_{m_2}} = \overline{T_h} + \frac{\overline{m_0}\ \overline{E}\,\overline{g}^{\,n+1}\,\overline{\gamma}\ d_n}{\overline{h}^{\,2n}};\ -\overline{x_1} \le \overline{x} \le \overline{x_2} \tag{19}$$

Where $d_n = \frac{n}{4(6n+1)}$;

Load and Traction

The load component in x-direction is given by

$$w_x = -\int_{h_1}^{h_2} p\,dh = -2\int_0^h p\,dh = \frac{1}{R}\int_{-\infty}^{x_2} x^2\,\frac{dp}{dx}\,dx \tag{20}$$

The dimensionless load $\overline{w_x} = \frac{W_x\alpha}{2h_0}$ is given by

$$\overline{w_x} = \int_{-\infty}^{\overline{x_2}} \overline{x}^{\,2}\,\frac{d\overline{p}}{d\overline{x}}\,d\overline{x} \tag{21}$$

The load component in y-direction is given by

$$w_y = \int_{-\infty}^{x_2} p\, dx \tag{22}$$

The dimensionless load $\overline{w_y} = \frac{W\alpha}{\sqrt{2Rh_0}}$ is calculated as

$$\overline{w_y} = \int_{-\infty}^{\overline{x_2}} \overline{x}\ \frac{d\overline{p}}{d\overline{x}}\, d\overline{x} \tag{23}$$

The load $\overline{W}$ is calculated by

$$\overline{W} = \sqrt{\overline{w}_x^{\,2} + \overline{w}_y^{\,2}} \tag{24}$$

Traction can be defined as the friction between drive wheel and the surface it moves upon. It is the amount of force a wheel can apply to a surface before it slips. Hence, the surface traction force $T_F h$, obtained from the integration of shear stress τ over the entire length , may be written as

$$T_{Fh} \;=\; \int_{-\infty}^{x_2} \left(\frac{h}{2} \left(\frac{dp}{dx} \right) \right)\, dx \tag{25}$$

Then, the dimensionless traction may be written as

$$\overline{T_{Fh}} \;=\; \int_{-\infty}^{\overline{x_2}} \overline{h}\ \left(\frac{d\overline{p}}{d\overline{x}} \right)\, d\overline{x}\,; \tag{26}$$

Finally, the consistency expression comes out to be

$$\overline{m} = \frac{\overline{m_0}\ \overline{E}\ \overline{h}^{\,2n}}{4^n\, \overline{y}^{\,2n}} \tag{27}$$

4. Results and Discussion

Thermal effect of fluid film lubrication of identical rollers by power law fluids under rolling and squeezing motions is studied. The lubricant consistency is encouraged to vary exponentially with pressure and the film temperature. The altered Reynolds and energy equations are derived and solved for pressure and temperature. For the numerical calculations the following set of values are used:
R = 0.03m; U = 4 m $\sec^{-1}$; α= 1.6 x$10^{-8}$$\mathrm{pa}^{-1}\mathrm{m}^2$; h_0= 6 x 10^{-5}m; $\overline{\gamma}$ = 4;
-0.1 < q < 0.1; 0.4 ≤ n ≤ 1.15 and 0 ≤ $\overline{T_h}$ - $\overline{T_0}$ ≤ 5;
The present paper attempts to show the consistency variation $\overline{m}$ of the lubricant

in a steady state thermal lubrication. Pressure $\overline{p}$, temperature $\overline{T}$, mean temperature $\overline{T_m}$ and velocity $\overline{u}$ are marked as functions of the power – law flow behavior index n, and squeezing parameter q. From the graph shown below, it can be interpreted that the variations in $\overline{p}$, $\overline{T_m}$ and $\overline{m}$ with $\overline{x}$ for various values of n and q do not change the general shape of the profile.

4.1. Pressure Distribution

The distribution of pressure $\overline{p}$ against $\overline{x}$ for various values of n for a fixed q, and for various values of q for a fixed n, are shown respectively in Fig. 2 & Fig. 3 and Fig. 4 & Fig. 5 for incompressible fluids in both thermal and iso-thermal cases. From the graph, it is possibly learnt that $\overline{p}$ increases continuously in the input region and decreases in the outlet region [20]. Once the pressure reaches the zenith, $\overline{p}$ falls down, making a steep slope in graph and reduces to the ambient pressure $\overline{p_2}$= 0 at the point of cavitation $\overline{x} = \overline{-x_2}$. The behavior of $\overline{p}$ against $\overline{x}$ for n (fixed) and varying q is similar to that of Dowson et al. [1].

For a fixed value of q, $\overline{p}$ increases significantly with n, especially when n is greater than or equal to 1. It is observed that fixed q value brings both the points of cavitation and maximum pressure nearer to the centre line of contact, (the origin 0) as n increases. Fixed n value increases $\overline{p}$ considerably as q decreases and the cavitation points move slowly towards the centre line of contact as q increases [21]. The change in pressure with respect to q accounts for the observation that as the surfaces approach each other, comparatively more pressure is generated. Maximum pressure with velocity is presented in Fig. 6 and Fig. 7 which are similar to the work done by Yu Chen et al [22].

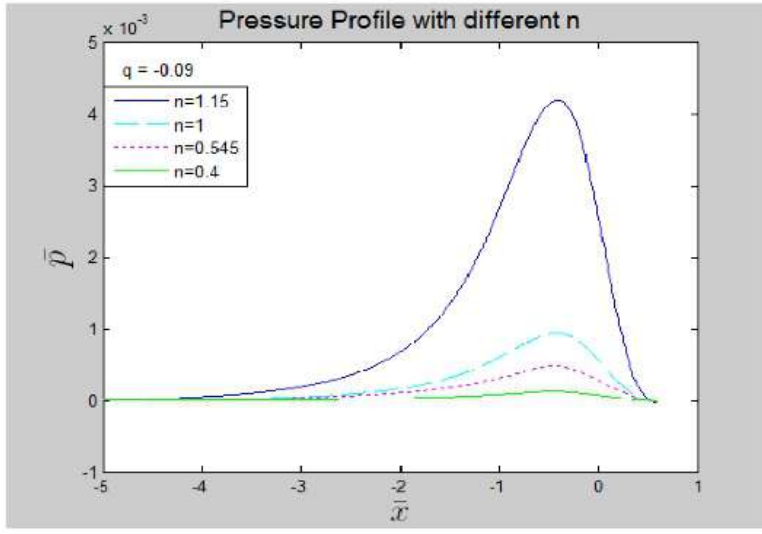

Fig.2: $\bar{p}$ Vs $\bar{x}$

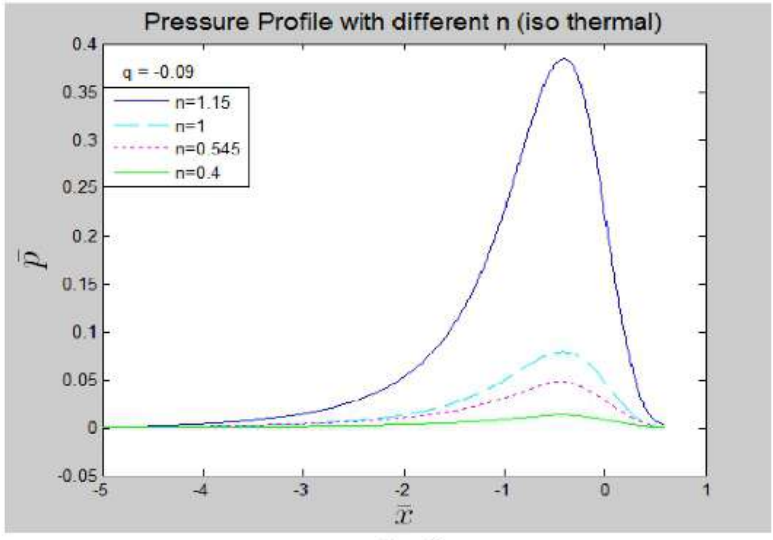

Fig.3: $\bar{p}$ Vs $\bar{x}$

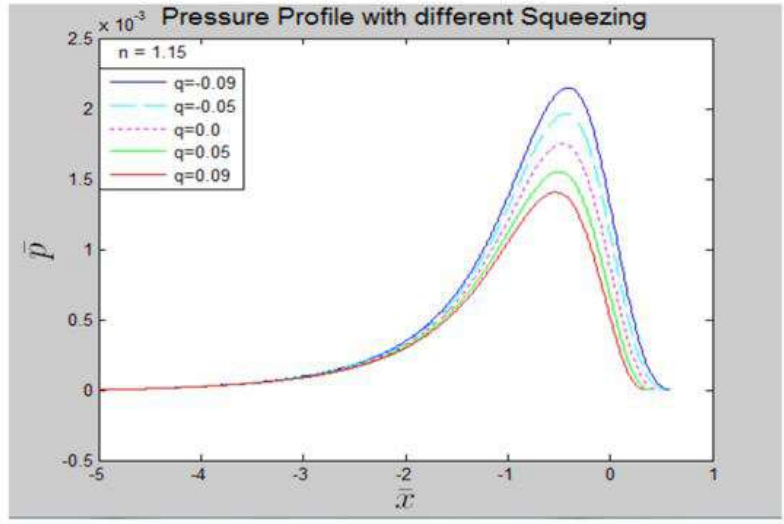

Fig.4: $\bar{p}$ Vs $\bar{x}$

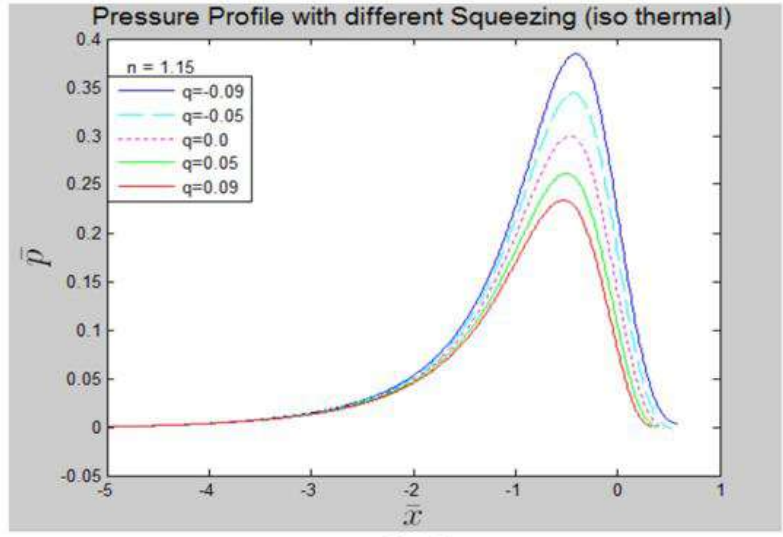

Fig.5: $\bar{p}$ Vs $\bar{x}$

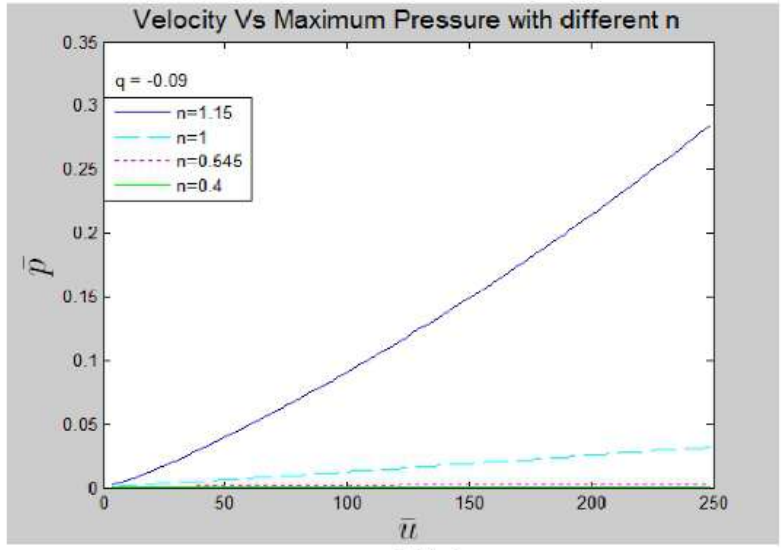

Fig.6: Max $\bar{p}$ Vs $\bar{u}$

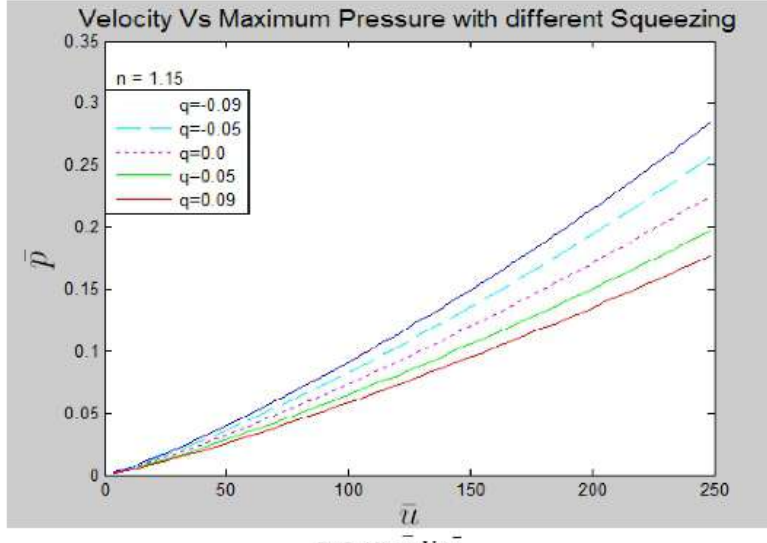

Fig.7: Max $\bar{p}$ Vs $\bar{u}$

4.2. Temperature Distribution

The mean temperature distribution $\overline{T_m}$ according to the n values is shown in Fig. 8 and Fig. 9. It is noteworthy to understand that mean temperature $\overline{T_m}$ increases in inner area. And the increase is ceased at the maximum pressure point, $\overline{x} = \overline{-x_1}$ and then $\overline{T_m}$ comes down slowly to the outer region. The increase $\overline{T_m}$ in the inner area is because of the dragging action of the faster layers in the high-pressure region generates more viscous dissipation in the convergence zone and results in more temperature [23]. From Fig. 8, it is learnt that $\overline{T_m}$ increases with n [21, 24, 25]. An increase in n denotes an enhanced effective viscosity. This increases the resistance to the motion, leading to a higher viscous dissipation. Similarly, $\overline{T_m}$ increases as q decreases with fixed n. The similar trend was also reported earlier [21]. Mean temperature- velocity graph is given in Fig.10 which is similar to that of Yu Chen et al [22]. A two dimensional temperature $\overline{T}$ profiles for a fixed n and q is given in Fig. 11.

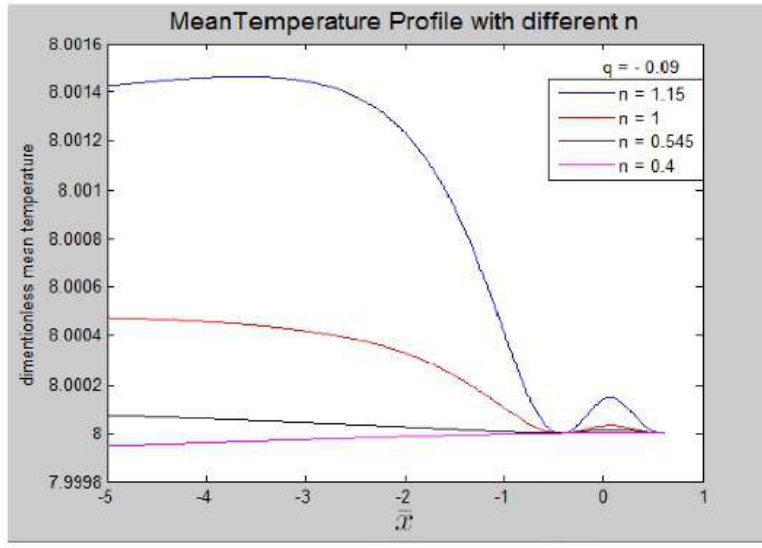

Fig.8: $\bar{T}_m$ Vs $\bar{x}$

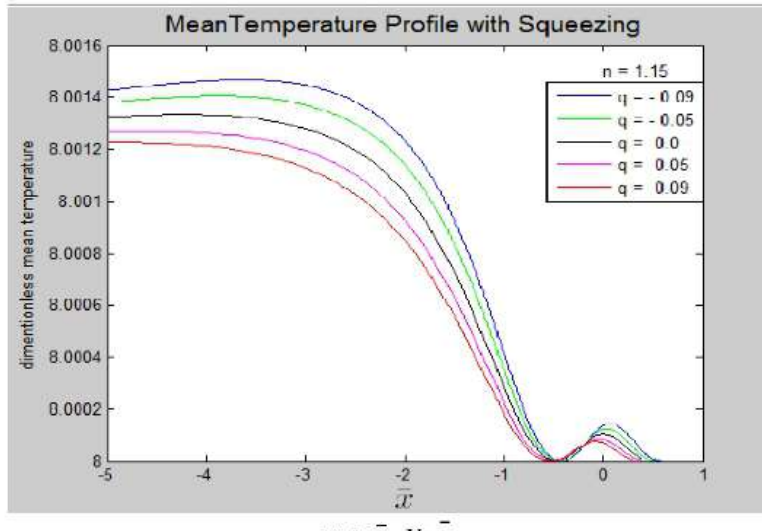

Fig.9: $\bar{T}_m$ Vs $\bar{x}$

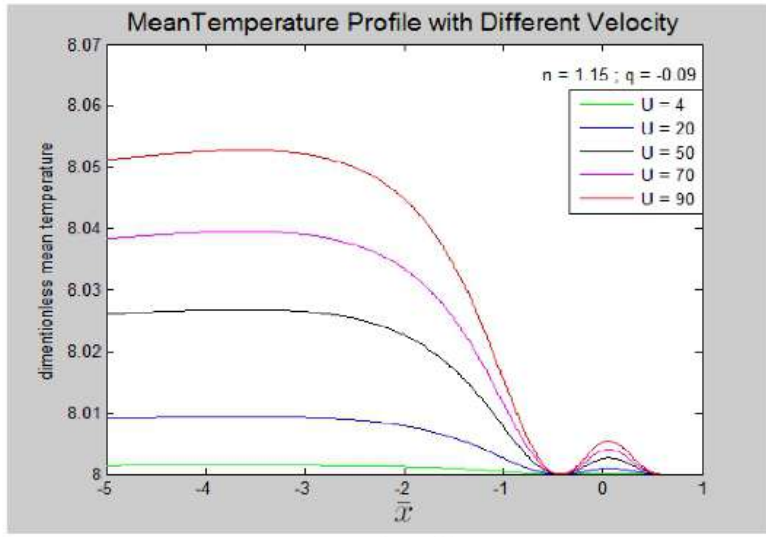

Fig.10: $\bar{T}_m$ Vs $\bar{x}$

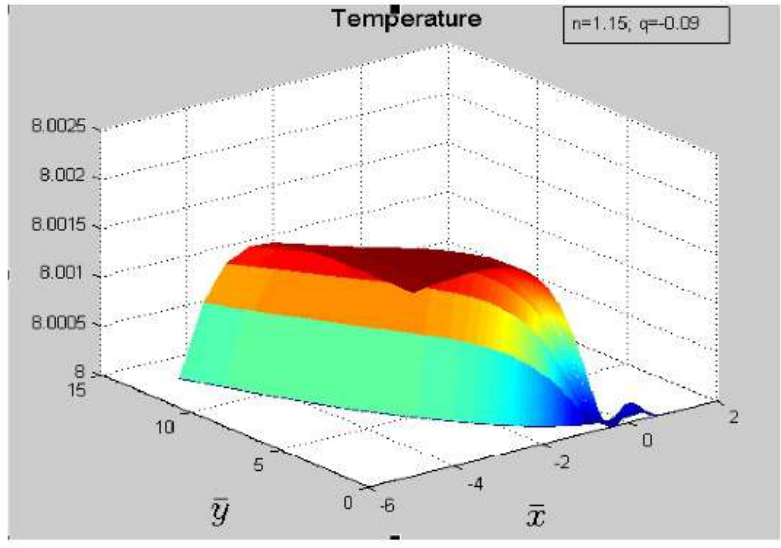

Fig.11: $\bar{T}$ Vs ($\bar{x}$ and $\bar{y}$)

4.3. Load and Traction

Load capacity and traction force are the salient features of bearings. It is presented in Table-1 with different n and q values for thermal conditions only. From the table it can be clearly stated that both the load $\overline{W}$ and the traction force $\overline{T}_{F_h}$, increases with n, which is in accordance with the previous findings [6, 21] for symmetric rollers and [13, 14] for asymmetric rollers, and the coefficient of traction decreases with n. Load versus speed graphs, given in Fig. 12 & Fig. 13, and are similar to the result of Yu Chen et al [22].

Table:1

n / m_0	q=-0.09	q=-0.05	q=0.00	q=0.05	q=0.09
x_1 values					
1.15/0.56	0.418464	0.440518	0.471939	0.503947	0.531958
1.00/0.75	0.420000	0.441891	0.474049	0.505410	0.534398
0.545/86.0	0.424184	0.445567	0.480227	0.508814	0.541901
0.40/128.0	0.427138	0.445961	0.480836	0.508454	0.542826
x_2 values					
1.15/0.56	0.598464	0.540518	0.471939	0.403947	0.351958
1.00/0.75	0.600000	0.541891	0.474049	0.405410	0.354398
0.545/86.0	0.604184	0.545567	0.480227	0.408814	0.361901
0.40/128.0	0.607138	0.545961	0.480836	0.408454	0.362826

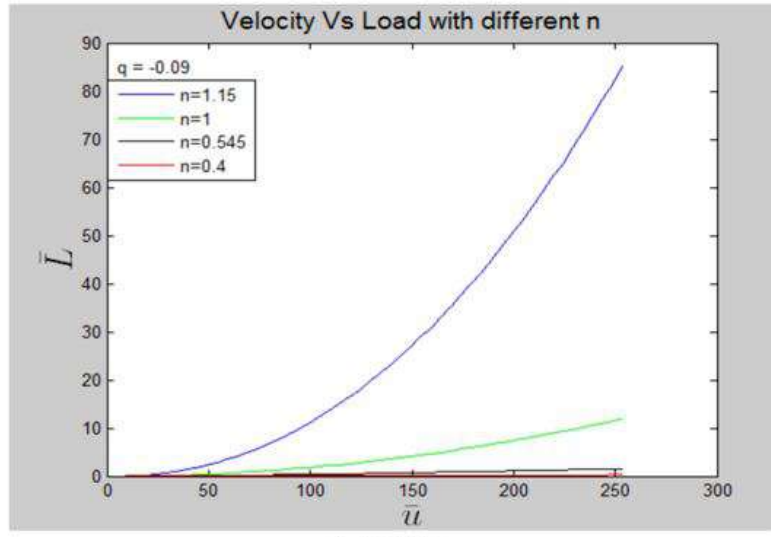

Fig.12: $\bar{L}$ Vs $\bar{u}$

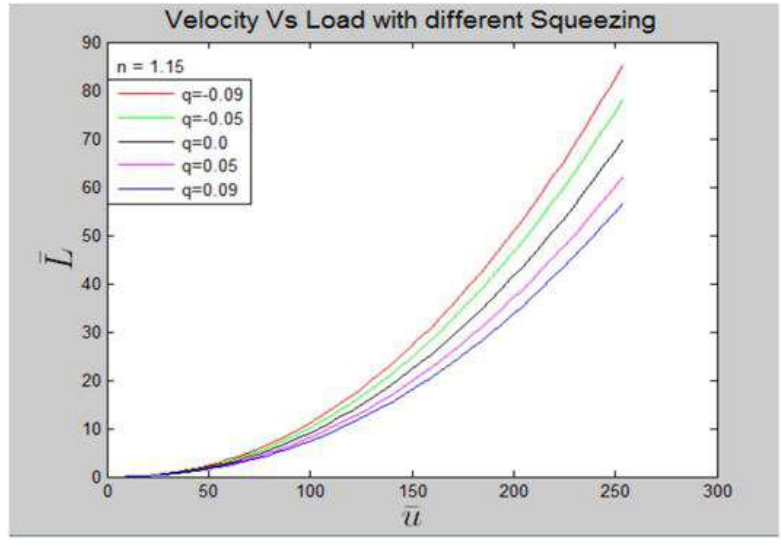

Fig.13: $\bar{L}$ Vs $\bar{u}$

Table: 2

$n\ /\ m_0$	q=-0.09	q=-0.05	q=0.00	q=0.05	q=0.09
Tangential load					
1.15/0.56	0.005246	0.005010	0.004713	0.004425	0.004195
1.00/0.75	0.001315	0.001266	0.001202	0.001140	0.001088
0.545/86.0	0.000970	0.000953	0.000929	0.000904	0.000882
0.40/128.0	0.000291	0.000288	0.000283	0.000277	0.000272
Normal load					
1.15/0.56	0.003119	0.002860	0.002554	0.002277	0.002076
1.00/0.75	0.000758	0.000702	0.000633	0.000571	0.000525
0.545/86.0	0.000503	0.000479	0.000447	0.000416	0.000393
0.40/128.0	0.000146	0.000140	0.000132	0.000124	0.000118
Load					
1.15/0.56	0.006103	0.005769	0.005360	0.004977	0.004681
1.00/0.75	0.001518	0.001447	0.001358	0.001275	0.001208
0.545/86.0	0.001092	0.001066	0.001031	0.000995	0.000965
0.40/128.0	0.000326	0.000320	0.000312	0.000304	0.000297
Traction					
1.15/0.56	0.005221	0.005001	0.004694	0.004427	0.004188
1.00/0.75	0.001310	0.001264	0.001196	0.001141	0.001084
0.545/86.0	0.000969	0.000955	0.000932	0.000908	0.000880
0.40/128.0	0.000290	0.000289	0.000286	0.000279	0.000273
Co-efficient of Traction					
1.15/0.56	0.855425	0.866792	0.875809	0.889533	0.894670
1.00/0.75	0.863184	0.873468	0.880952	0.895066	0.897378
0.545/86.0	0.887202	0.896060	0.903870	0.911924	0.911129
0.40/128.0	0.890755	0.903815	0.914467	0.916847	0.918300

4.4. Consistency

The main feature of this article is to study two-dimensional change in the consistency $(\overline{m})$ of the power law fluids with pressure and the two-dimensional temperature as shown in the below figures. The overall consistency changes with $\overline{x}$ at different positions of the lubricant heights above the x-axis is shown in Fig. 14: This indicates basically the dominance of temperature over the pressure (refer the equation number (27)). Further, $(\overline{m})$ changes enormously with $\bar{}$y. This shows that changes much near the symmetric line of the two cylinders and least near the moving surfaces. The consistency versus speed curve is given in Fig.15, and is similar to the result of Espejel [23]. A one dimensional consistency variation in $(\overline{m})$ with $(\overline{x})$ for different flow index n is given in Fig. 16, and a two dimensional variation is shown in Fig. 17. Hence, the consideration of the consistency variation with pressure and temperature is well justified.

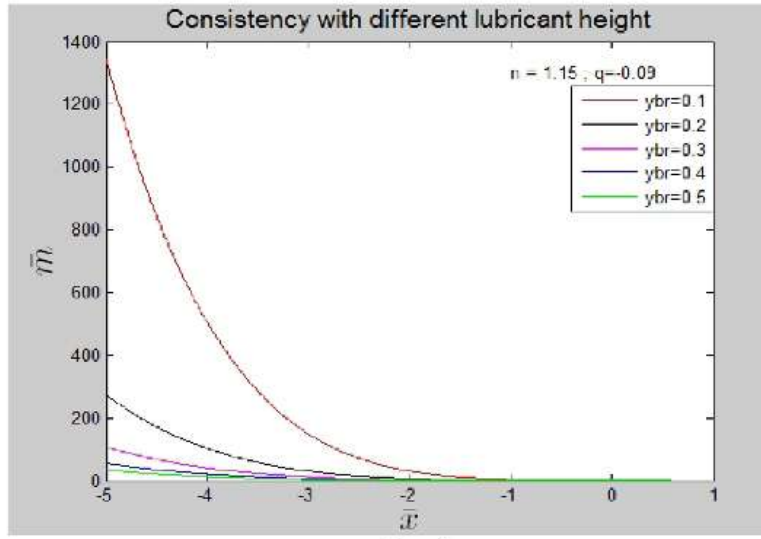

Fig.14: $\bar{m}$ Vs $\bar{x}$

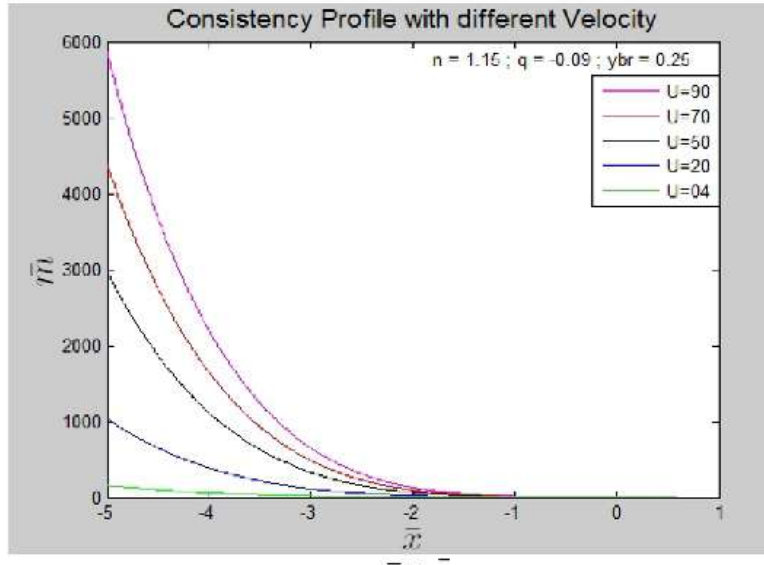

Fig.15: $\bar{m}$ Vs $\bar{x}$

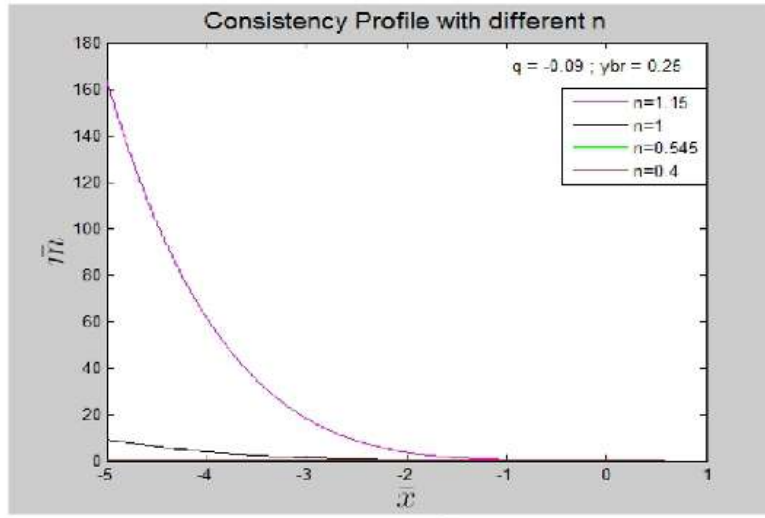

Fig.16: $\bar{m}$ Vs $\bar{x}$

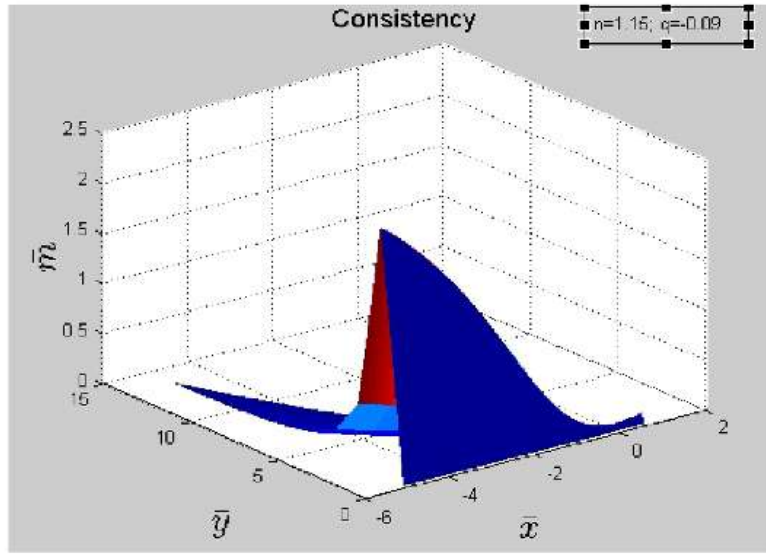

Fig.17: $\bar{m}$ Vs ($\bar{x}$ and $\bar{y}$)

5. Conclusion

To study the consistency variation $\overline{m}$ of the power law fluids, a two dimensional temperature $\overline{T}$ is incorporated to the flow index n and the squeezing parameters q. To analyze the effects of pressure and temperature on the consistency $\overline{m}$ of the fluids, a descriptive method is adopted. Loads and tractions are also studied along with consistency variation. It is found that the pressure and the corresponding temperature increase with n and decrease as q increases numerically. The point of pressure peak moves away from the centre line of contact as q increases. The same trend of pressure with q and n is seen with load and traction. A two-dimensional temperature profile and consistency variation curves are also drawn for some fixed values of n and q which are expectedly nowhere found in the literature. These are the following important observations:

* $\overline{T}, \overline{p}$, n and q are incorporated to observe the consistency variation $\overline{m}$ of the power law fluids.
* Descriptive/ semi-analytical method is adopted for the study of the effects of pressure and temperature on consistency.
* Besides consistency variation, load and traction are also reviewed.
* It is observed that the temperature and pressure upsurge with n and downfalls as q rises numerically. As q increases, the pressure point sidelines from the center line of contact.
* Load and traction exhibit a similar pattern of pressure with q and n.
* For fixed values of n and q, two dimensional consistency variation along with temperature curves are drawn.
* The results are in natural agreement with the previous findings.

References

[1] Dowson, D., Markho, P. H., Jones, D. A., The lubrication of lightly loaded cylinders in combined rolling, sliding and normal motion - Part I, Theory. J. Lub. Techn., 98(1976), 509.

[2] Rong - Tsong, L., Hamrock, B. J., Squeezing and entraining motion non-conformal line contacts, part - I, J. Tribol, 111(1989), 1-7.

[3] Usha, R., Rukmani Sridharan, An investigation of a squeeze film between two plane annuli, J. Tribol, 120(1988), 610-615.

[4] Cheng, H. S., Sternlicht, B., A numerical Solution for the Pressure, Temperature and Film Thickness Between Two infinite Long Lubricated Rolling and Sliding Cylinders Under Heavy Loads, J. of Basic Engg., 87(1965), 695-707.

[5] Ghosh M. K., Hamrock, B. J., Thermal EHD Lubrication of Line Contacts, 28(1985), 159-171.

[6] Dhaneshwar Prasad and Chhabra, R. P., Thermal and normal squeezing effects lubrication of rollers by a power law fluid, Wear, 145(1991), 61-76 .

[7] Neurouth, A., Changenet, C., Ville, F., Thermal modeling of a grease lubricated thrust ball bearing, Proc. Inst. Mech. Eng. Part J, J. Eng. Tribol, 228(2014), 1266–75.

[8] Ai, S. Y., Wang, W. Z., Wang, Y. L., Temperature rise of double-row tapered roller bearings analyzed with the thermal network method, Tribol Int., 87(2015), 11–22.

[9] Yan, K., Wang, N., Zhai, Q., Theoretical and experimental investigation on the thermal characteristics of double-row tapered roller bearings of high speed locomotive, Int. J. Heat Mass Transf., 84(2015), 1119–1130.

[10] Fangbo Ma, Zhengmei Li, Shengchang Qiu, Baojie Wu, Qi An., Transient thermal analysis of grease-lubricated spherical roller bearings, Tribol. Int., 93(2016), 115–123.

[11] Osterle, F., Saibel, E., On the Effect of Lubricant Inertia in Hydrodynamic Lubrication, Z. Angew. Math. U. Phys., 6(1955), 334.

[12] Cameron, A., Basic Lubrication Theory, Ellis Harwood Limited, coll. House, Watergate, Chicester, (1981), 45-162.

[13] Dhaneshwar Prasad and Venkata Subrahmanyam Sajja, Non-Newtonian Lubrication of Asymmetric Rollers with Thermal and Inertia Effects, Tribol. Trans., 59(2016), 818-830.

[14] Dhaneshwar Prasad and Venkata Subrahmanyam Sajja, Thermal Effect in non - Newtonian Lubrication of Asymmetric Rollers Under Adiabatic and Isothermal Boundaries, Int. J. Chem. Sci., 14(2016), 1641-1656.

[15] Gao W, Nelias D, Lyu Y, Boisson N., Numerical investigations on drag coefficient of circular cylinder with two free ends in roller bearings, Tribol Int., 123(2018), 43–9.

[16] Wenjun Gao, Daniel Nelias, Kun Li, Zhenxia Liu, Yaguo Lyu, A multiphase computational study of oil distribution inside roller bearings with under-race lubrication, Tribology International 140(2019), 105862.

[17] Dhaneshwar Prasad, Nagarajan, V., Analytical Solution for Lubrication of Rollers by Power law fluids with Thermal effect including Cavitations, Nat. Conf. Adv. Math. and its Applications (CAMA'11), Bathinda, India, (2011), 109-115.

[18] Aftab Ahmed, Jabed I, Siddique and Muhammad Sagheer, Dual solutions in a boundary layer flow of a power law fluid over a moving permeable flat plate with thermal radiation, viscous dissipation and heat generation –absorption, MDPI, Fluids. 3, 6 (2018).

[19] Dhaneshwar Prasad , Punyatma Singh, Prawal Sinha, Thermal and Squeezing Effects in Non-Newtonian Fluid Film Lubrication of Rollers, Wear, 119(1987), 175 - 190.

[20] Hajishafiee, A., Kadiric, A., Ioannides, S., Dini, D., A coupled finite volume CFD solver for two dimensional EHL problems with particular application to rolling element bearings, Tribology international. 109(2017), 258-273.

[21] Sinha, P., Prasad, D., Lubrication of rollers by power law fluids considering consistency variation with pressure and temperature, Acta Mechanica, 111(1995), 223-239.

[22] Yu Chen, Yu Sun, Qiang He, Jun Feng., EHD behavior analysis of journal bearing using fluid structure interaction considering cavitation, Arabian J. Sci. Engg, doi.org/10.1007/s 13369-018-3467-9 (2018).

[23] Morales-Espejel, G. E., Lugt, P. M., Pasaribu H. Cen, H. R., Film thickness in grease lubricated slow rotating rolling bearings. Tribol. Int, 74(2014), 7-19.

[24] Fangbo Ma, Zhengmeili, Shengchang Qiu, Baojie Wu and Qi An, Transient thermal analysis of grease lubricated spherical roller bearings, Tribol. Int., 93(2016), 115-123.

[25] Gabriella Bognár, János Kovács., Non-Isothermal Steady Flow of Power-Law Fluids between Parallel Plates, Int. J. Math. Models and Methods in Appl. Sci., 6(2012), 122-129.